

Establishment of a miRNA-mRNA regulatory network in metastatic renal cell carcinoma and screening of potential therapeutic targets

Jie Zhu¹ · Xin Ma¹ · Yu Zhang¹ · Dong Ni¹ · Qing Ai¹ · Hongzhao Li¹ · Xu Zhang¹

Received: 17 February 2016 / Accepted: 6 July 2016 / Published online: 2 November 2016
© International Society of Oncology and BioMarkers (ISOBM) 2016

Abstract This study aimed to screen effective diagnosis or treatment biomarkers for renal cell carcinoma, especially for metastatic renal cell carcinoma (mRCC) based on microRNA (miRNA) and messenger RNA (mRNA) genechip, and their regulatory network. The differential expressions of miRNAs and mRNAs were examined by miRNA and mRNA genechip analyses, respectively, in patients with either localized renal cell carcinoma (IRCC) or mRCC, and a miRNA-mRNA regulatory network was established. Subsequently, the regulation of selected mRNAs by miRNAs was validated by reverse transcription-quantitative polymerase chain reaction (RT-qPCR) and dual-luciferase reporter gene assay. Thirty-one up-regulated miRNAs, 196 down-regulated miRNAs, 214 up-regulated mRNAs, and 156 down-regulated mRNAs were identified in patients with mRCC. In total, 1315 miRNA-mRNA pairs, involving 34 miRNAs and 225 mRNAs, were established. The expression profiles of four up-regulated miRNAs, hsa-miR-139-5p, hsa-miR-140-3p, hsa-miR-151a-3p, and hsa-miR-204-5p, and four down-regulated miRNAs, hsa-miR-409-3p, hsa-miR-671-3p, hsa-miR-1203, and hsa-miR-1290, were consistent with the results from the miRNA gene-chip analysis. The expression profiles of *NEU2*, *MASPI*, *MCL1*, *ARHGAP11A*, *HOXA1*, and *CLDN8* were consistent with the results from the mRNA gene-chip analysis. In vitro, hsa-miR-140-3p bound to the 3' untranslated region (3'-UTR) of the *MASPI* mRNA and down-regulated its expression. Similarly, hsa-miR-151a-

3p, hsa-miR-671-3p, and hsa-miR-1290 bound to the 3'-UTRs of the *MCL1*, *HOXA1*, and *HOXA1* mRNAs, respectively, and down-regulated their expressions. However, binding by hsa-miR-140-3p, hsa-miR-671-3p, or hsa-miR-1290 did not down-regulate the expressions of *NEU2*, *ARHGAP11A*, and *CLDN8*, respectively. This study provides a significant reference of investigating the pathogenesis of mRCC and the subsequent screening of potential therapeutic targets.

Keywords Localized renal cell carcinoma · Metastatic renal cell carcinoma · Genechip · Regulatory network · Molecular target · Screening

Introduction

Renal cell carcinoma, a malignancy that originates from the tubular epithelial system of the renal parenchyma, is the seventh most prevalent tumor in males and the tenth most prevalent tumor in females and severely affects human health and society [1, 2]. According to the 2010 American Joint Committee on Cancer report on the Classification of Malignant Tumors, an optimal therapeutic schedule was developed based on combined imaging procedures and clinical staging and ensured extensive analysis of tumor invasion and postoperative treatment based on postoperative histopathology [3]. Usually, non-metastatic renal cell carcinoma is treated through surgical resection, which results in a good prognosis and a 5-year survival rate of 70 %. However, approximately 20–40 % of non-metastatic renal cell carcinomas are locally recurrent or undergo metastasis [4, 5]. After renal cell carcinoma metastasizes, peripheral tissues may undergo severe organic lesions and failure, and there may be the onset of severe multi-organ dysfunction syndrome. The median survival time after metastasis is just 12 months, and the 5-year survival rate

Jie Zhu and Xin Ma contributed equally to this work.

✉ Xu Zhang
xzhang@foxmail.com

¹ Department of Urology, Chinese People's Liberation Army General Hospital, Beijing 100853, China

is less than 10 % [6, 7]. Metastatic renal cell carcinoma (mRCC) is clinically classified as stage IV [8, 9]. It is a severe malignant disease that develops rapidly, is associated with high mortality, is poorly responsive to chemoradiotherapy, and has no standard treatment regimen. Surgery is not the optimal treatment for mRCC, and traditional drugs, such as interleukin-2 and/or interferon- α , do not provide a curative effect for the majority of patients [10]. With growing understanding of the pathogenesis of renal cell carcinoma, a number of small-molecule drugs that recognize different molecular targets have been developed to effectively improve the survival rate of patients with advanced mRCC. These small molecule drugs include the multi-target inhibitors sorafenib and sunitinib, the VEGF inhibitor bevacizumab, and the mTOR inhibitors everolimus and sirolimus. Importantly, with the development of gene-chip microarrays and next-generation DNA sequencing, small molecules that target microRNAs (miRNAs) have become a major focus of studies and will likely become a novel approach for treating cancer [11–14].

miRNAs are endogenous, non-coding, small RNAs of 21–25 nucleotides and are widely distributed in tissues and organs of different species. miRNAs strongly affect their target genes by forming RNA-induced silencing complexes (RISCs) that partially bind to the 3' untranslated region (3'-UTR) of target genes to induce messenger RNA (mRNA) degradation or to inhibit mRNA translation [15, 16]. So far, about 2000 miRNAs have been identified in the human genome and regulate over 30 % of the total genome [17]. miRNAs mainly regulate the physiology and development of tissues and can induce changes in cell proliferation, cell cycle, apoptosis, cell migration and invasion, and angiogenesis. Altered miRNA expression could be a useful target for the early diagnosis and treatment of renal cell carcinoma [18]. Juan et al. have identified 9 up-regulated miRNAs and 26 down-regulated miRNAs in renal carcinoma, of which 10 miRNAs could potentially be used for identifying renal carcinoma [19]. From gene-chip analysis, 38 up-regulated and 48 down-regulated miRNAs were identified in renal carcinoma [20]. Several other studies have shown significant changes in miRNAs that could be used as biomarkers for the diagnosis of renal carcinoma [21–23]. Importantly, Butz et al. have constructed a miRNA-mRNA network of clear cell renal cell carcinoma (ccRCC), and identified 600 miRNA-mRNA interaction pairs involving 49 miRNAs and 266 genes, and further conformed that miR-124 as a key miRNA contributing to ccRCC aggressive behavior by targeting CAV1 and FLOT1 [24]. However, the differential expressions of miRNAs and mRNAs in mRCC, particularly in studies that explore the miRNA-mRNA regulatory network and its potential clinical application, have not been reported. Therefore, in the present study, differentially expressed miRNAs and mRNAs were identified by miRNA and mRNA gene-chip analyses, and the miRNA-mRNA regulatory network was identified and validated by

reverse transcription-quantitative polymerase chain reaction (RT-qPCR) and by luciferase assays using a dual-luciferase reporter system. As expected, several differentially expressed miRNAs and mRNAs, and the resulting miRNA-mRNA regulatory network, were identified and provided potential candidates for the diagnosis and treatment of renal carcinoma, especially mRCC.

Materials and methods

Patients and groups

For the miRNA gene-chip assay, a total of 28 patients with renal carcinoma, who were hospitalized between February 2010 and December 2013, and diagnosed with renal clear cell carcinoma, were randomly divided into two groups according to the metastatic status of their renal carcinoma and the tumor node metastasis classification system [25, 26]; these included 13 cases of localized renal cell carcinoma (IRCC) and 15 cases of mRCC. Similarly, for the mRNA gene-chip assay, a total of 10 patients with renal carcinoma were randomly divided into two groups; these included five cases of IRCC and five cases of mRCC. The IRCC group and the mRCC group did not differ in mean age or gender distribution of the patients, and all provided written consent to participate in this study, which was approved by the Ethics Committee of the Chinese People's Liberation Army General Hospital.

miRNA extraction and miRNA gene-chip assay

A total of 100-mg renal tissue from patients with IRCC or mRCC was frozen in liquid nitrogen and ground to facilitate extraction of miRNAs using TRIzol reagent (Invitrogen, USA), according to the manufacturer's instructions. After grinding, 1 mL of TRIzol was added, and the samples were mixed for 30 s and then incubated at room temperature for 5 min. Chloroform (200 μ L; Invitrogen, USA) was added to the samples, which were mixed for 15 s; incubated at room temperature for 5 min; and centrifuged at 4 $^{\circ}$ C, at 12,000 rpm for 10 min. The supernatant was collected, mixed with 1.5 v of absolute ethanol (Sinopharma Chemical Reagent Co. Ltd., Shanghai, China), transferred to a miRspin column, and centrifuged at room temperature, at 12,000 rpm for 30 s. The effluent was removed, and 500 μ L MRD buffer was added to the column, which was incubated at room temperature for 2 min, followed by centrifugation at room temperature, at 12,000 rpm for 30 s. The effluent was removed and 700 μ L RW buffer was added to the column, which was incubated at room temperature for 2 min, followed by centrifugation at room temperature, at 12,000 rpm for 30 s. This step was repeated once with 700 μ L RW buffer. The effluent was removed and 500 μ L RW buffer was added to the column,

which was then incubated at room temperature for 2 min, followed by centrifugation at room temperature, at 12,000 rpm for 30 s. The column was transferred to a new collection tube and centrifuged at 12,000 rpm for 1 min to remove any residual liquid. After air-drying at room temperature, 30 μ L of RNase-free double-distilled H₂O (dd H₂O) was added to the miRspin column. The column was centrifuged at room temperature, at 12,000 rpm for 2 min. The effluent was collected, and the concentration and purity of the miRNA were determined by ultraviolet spectrophotometry. The MRA-1001LCB_miRHuman_20 gene chip was assayed as follows: the miRNA was fluorescently labeled using T4 RNA ligase (TaKaRa, Japan) and precipitated by absolute ethanol (Sinopharma Chemical Reagent Co. Ltd., Shanghai, China). The miRNA was added to 16 μ L of hybridization solution and allowed to hybridize to the chip at 42 °C overnight. The chip was washed with $\times 2$ saline sodium citrate (SSC) at 42 °C for 4 min and then with $\times 0.2$ SSC at room temperature for 4 min. The fluorescent signal was detected with a LuxScan 10 K-A dual-channel laser scanner, and differential miRNA expression was assigned according to Student's *t* test and the fold change (FC) using the Significance Analysis of Microarrays (SAM version 2.1) software, wherein FC was defined as the ratio of the average expression of an miRNA in patients with mRCC/the average expression of the miRNA in patients with IRCC, and considered to be differentially expressed at $p < 0.05$, with up-regulation of its gene if $FC \geq 2$ or down-regulation if $FC \leq 0.5$.

mRNA extraction and mRNA gene-chip assay

A total of 100-mg renal tissue from patients with IRCC or mRCC was frozen in liquid nitrogen and ground to facilitate the extraction of mRNAs with TRIzol, following the manufacturer's instructions. After grinding, 1 mL of TRIzol was added, followed by mixing for 30 s, and samples were incubated at room temperature for 5 min, followed by centrifugation at 4 °C, at 12,000 rpm for 10 min. The supernatant was collected and 200- μ L chloroform was added and mixed for 15 s, and then, the sample was incubated at room temperature for 3 min, followed by centrifugation at 4 °C, at 12,000 rpm for 15 min. An equal volume of isopropyl alcohol was mixed with the absorbed aqueous phase, which was incubated at room temperature for 30 min then centrifuged at 4 °C, at 12,000 rpm for 10 min, and the supernatant was removed. The pellet was washed in 1 mL, 75 % ethanol, centrifuged at 4 °C, at 5000 rpm for 3 min, and (after removal of residual liquid) air-dried at room temperature. After addition of 100 μ L RNase-free ddH₂O and centrifugation at room temperature, at 12,000 rpm for 2 min, the effluent was collected, and the concentration and purity were examined by ultraviolet spectrophotometry. The Affymetrix

GeneChip Human Genome U133 Plus 2.0 Array was assayed as follows: the mRNA was fluorescently labeled using T₄ RNA ligase and precipitated by absolute ethanol. The labeled mRNA was added to 16 μ L hybridization solution and allowed to hybridize to the chip at 42 °C overnight. The chip was washed with $\times 2$ SSC at 42 °C for 4 min and then with $\times 0.2$ SSC at room temperature for 4 min. The fluorescent signal was detected with a LuxScan 10 K-A dual-channel laser scanner, and differential mRNA expression was assigned according to Student's *t* test and the fold change (FC) using the SAM (version 2.1) software, wherein FC was defined as the ratio of the average expression of mRNA in patients with mRCC/the average expression average mRNA in patients with IRCC, and considered to be differentially expressed at $p < 0.05$, with up-regulation of its gene if $FC \geq 2$ or down-regulation if $FC \leq 0.5$.

Gene ontology clustering

The gene ontology (GO) database (<http://geneontology.org/>) includes the following three functional categories: biological process, cellular component, and molecular function. Genes could be further organized by directed acyclic graph according to their scope. In GO clustering, genes are considered significantly enriched based on the ratio of the observed GO term for all genes/GO term for a single gene set. First, each gene that was assigned a particular GO term was broadly noted in the upper father node, then the *p* value of each enriched GO term was determined using a hypergeometric distribution, and the *p* value was adjusted using the false discovery rate (FDR), with $p = 0.05$ selected as the threshold value. Subsequently, redundant GO terms were removed, and the hierarchy chart's terminal nodes were selected as the final significantly enriched GO terms.

Kyoto Encyclopedia of Genes and Genomes pathway enrichment analysis

The Kyoto Encyclopedia of Genes and Genomes (KEGG) database (<http://www.genome.jp/kegg/pathway.html>) is used to systematically analyze gene function and genomic information from biological pathways and to further group biological pathways according to metabolism, enzyme, biochemical reaction, gene regulation, and protein–protein interaction. Here, KEGG signaling pathway analysis was applied, followed by hypergeometric distribution analysis and the FDR method to give an adjusted *p* value ($p = 0.05$ as a threshold value). To identify the KEGG signaling pathway for differentially expressed miRNAs or mRNAs, we carried out KEGG pathway enrichment of their up-regulated or down-regulated genes.

miRNA-mRNA regulatory network

miRNAs and their target genes were initially predicted using the miRanda, PicTar, microRNA.org, PITA, RNA22 microRNA target detection, and TargetScanS algorithms, and target genes were verified using the TarBase database. Thus, a hub miRNA was defined as having a connectivity ≥ 10 . A hub miRNA and its regulated genes were then classified to a hub-miRNA module as follows: opposite modes of regulation of miRNAs and mRNAs were identified based on their expression profiles and used to determine each miRNA-mRNA and miRNA-target intersection. High reliability for the miRNA-target intersection was used to establish the hub-miRNA module and to predict target-gene function in the hub-miRNA module. Subsequently, an overall network was established based on verified protein-protein interactions using the STRING database and miRNA targets. Visual representations of interaction webs were designed and constructed using the Cytoscape software and the igraph data package on an R platform. Finally, a closed connected network module was identified using the Markov cluster algorithm, a module of ≥ 10 nodes was selected, and then the enriched GO and KEGG pathway terms were identified in each network module.

Quantitative reverse transcription-polymerase chain reaction assay of miRNA

miRNA was used as the template in a reverse transcription reaction using a kit (TOYOBO, Japan), according to the manufacturer's instructions. The miRNA reverse transcription reaction mixture included 10 μL $\times 2$ loading buffer, 1.2 μL miRNA RT primer/U6 small nuclear RNA primer, 2 μL miRNA template, 0.2 μL MMLV reverse transcriptase, and 6.6 μL DEPC-treated H_2O . The reaction was incubated at 26 $^\circ\text{C}$ for 30 min, followed by 42 $^\circ\text{C}$ for 30 min, and then by 85 $^\circ\text{C}$ for 10 min. For quantitative PCR (qPCR), 100 ng complementary DNA (cDNA) was used as the template in a reaction mixture that included 10 μL $\times 2$ Master Mix, 0.08 μL forward primer, 0.08 μL reverse primer, 2 μL cDNA template, 0.4 μL Taq DNA polymerase, and 7.44 μL dd H_2O . The qPCR amplification conditions were as follows: 1 cycle of 95 $^\circ\text{C}$ for 3 min, 40 cycles of 95 $^\circ\text{C}$ for 12 s, 62 $^\circ\text{C}$ for 30 s, and 72 $^\circ\text{C}$ for 30 s. The results were analyzed using SDS 1.4 software (Applied Biosystems).

Quantitative reverse transcription-polymerase chain reaction assay of mRNA

mRNA was used as the template in a reverse transcription reaction using a kit (TOYOBO, Japan), according to the manufacturers' instructions. The mRNA reverse transcription reaction mixture included 10 μL $\times 2$ loading buffer, 1.2 μL oligo

(dT), 2 μL mRNA template, 0.2 μL MMLV reverse transcriptase, and 6.6 μL DEPC H_2O . The reaction was incubated at 26 $^\circ\text{C}$ for 30 min, followed by 42 $^\circ\text{C}$ for 30 min, and then by 85 $^\circ\text{C}$ for 10 min.

For qPCR, 100 ng cDNA was used as the template in a reaction mixture that included 10 μL $\times 2$ Master Mix, 0.08 μL forward primer, 0.08 μL reverse primer, 2 μL cDNA template, 0.4 μL Taq DNA polymerase, and 7.44 μL dd H_2O . The qPCR amplification conditions were as follows: 1 cycle of 95 $^\circ\text{C}$ for 3 min, 40 cycles of 95 $^\circ\text{C}$ for 12 s, 62 $^\circ\text{C}$ for 30 s, and 72 $^\circ\text{C}$ for 30 s. The results were analyzed using the SDS 1.4 software (Applied Biosystems), and a histogram was generated using the Origin 9.5 software (<http://www.originlab.com/>).

Construction of a dual-luciferase reporter-gene vector

The miRNA sequences were obtained from the miRBase database (<http://www.mirbase.org/>), and the complementary single strand was designed and synthesized for each. The full-length 3'-UTR of the target gene was conjugated to sites for the restriction endonucleases *EcoRI* (TaKaRa, Japan) and *XhoI* (TaKaRa, Japan). After restriction enzyme digestion, the target fragment was cloned into the psiCHECK-2 vector using T_4 DNA ligase and then used to transform competent *Escherichia coli* DH5 α cells (TaKaRa, Japan). A positive clone was selected and plasmids were extracted for direct sequencing.

Luciferase activity assay

For the luciferase activity assay, 293 T cells were plated 24 h prior to transfection to be 30–50 % confluent at the time of transfection and were divided into the following four groups: psiCHECK-2-UTR, psiCHECK-2-UTR/mimic, psiCHECK-2-UTR/inhibitor, and psiCHECK-2-UTR/mimic/inhibitor. A 2.5 μL mixture of the inhibitor and mimic/inhibitor plasmids and 50 ng of the luciferase reporter plasmid were added to 100 μL Opti-MEM medium. Lipofectamine 2000 reagent was diluted 1:50 with Opti-MEM medium, incubated for 5 min, mixed with the mimic miRNA and the luciferase reporter plasmid, and incubated for a further 20 min. The cells were washed with serum-free medium, which was then discarded, and then, 800 μL of serum-free medium was added to each well. The mixture was gently added to each well for transfection at 37 $^\circ\text{C}$ for 6 h and then replaced with fresh medium for a further 48 h of incubation. Cells were washed twice with phosphate-buffered saline (3 min each wash), and then, the cells were shocked by the addition of 100 μL $\times 1$ PLB buffer and incubated at room temperature for 15 min. Twenty microliters of PLB lysis buffer was absorbed to a detector tube that already contained 100 μL Luciferase Assay Reagent II. Subsequently, 100 μL Stop&Glo reagent was added to detect

the activity of *Renilla* luciferase. The ratio of firefly luciferase/*Renilla* luciferase was calculated, and histogram analysis was carried out using the Origin 9.5 software (<http://www.originlab.com/>).

Statistical analysis

All data are expressed as the mean \pm standard deviation (SD). Statistical analysis was carried out by one-way analysis of variance using the SPSS software (version 21.0; <http://spss.en.softonic.com/>). Student's *t* test was carried out on groups of two samples, and $p < 0.05$ and $p < 0.01$ were considered to indicate a significant difference and a highly significant difference, respectively.

Results

Identification of 31 up-regulated miRNAs and 196 down-regulated miRNAs by miRNA gene-chip analysis

As shown in Table 1, the and mRCC often occurred in male and reached 69.24 and 66.67 %, respectively, and had no difference in age and gender. According to the TNM staging, the IRCC patient was in T1, N0, and M0, and was divided into I stage, and that of mRCC patients was in T1, T2, N, and M1 and was divided into IV stage.

As indicated by miRNA gene-chip analysis, when compared to miRNAs from patients with IRCC, 31 miRNAs were up-regulated and 196 miRNAs were down-regulated in patients with mRCC. Table 2 shows the top 10 significantly up-regulated and the top 10 significantly down-regulated miRNAs. Based on the results of miRNA and mRNA cross-over network analysis, four up-regulated miRNAs, hsa-miR-139-5p, hsa-miR-140-3p, hsa-miR-151a-3p, and hsa-miR-204-5p, and four down-regulated miRNAs, hsa-miR-409-3p, hsa-miR-671-3p, hsa-miR-1203, and hsa-miR-1290, were chosen and analyzed for GO and KEGG pathway enrichment (Fig. 1). The hsa-miR-139-5p miRNA is associated with the biological processes of metabolism of norepinephrine, regulation of cell shape, determination of cell fate, negative regulation of cell proliferation, differentiation of epithelial cells, establishment of cell polarity, positive regulation of myeloid cell

Table 2 Differentially expressed miRNAs in patients compared mRCC with IRCC

miRNA	<i>p</i> value	Direction	FC
hsa-miR-642b-5p	0.037621	+	47.95818
hsa-miR-3154	0.038561	+	7.068793
hsa-miR-139-5p	8.71E-05	+	6.398992
hsa-miR-3944-3p	0.02933	+	5.342755
hsa-miR-4691-3p	0.046601	+	4.945863
hsa-miR-1237-3p	0.005014	+	4.37947
hsa-miR-2110	0.040616	+	3.982532
hsa-miR-1245a	0.001117	+	3.842558
hsa-miR-10b-3p	0.000877	+	3.370348
hsa-miR-1273 g-5p	0.015146	+	3.2614
.....
hsa-miR-891a-5p	0.001182	–	0.058813
hsa-miR-938	0.002509	–	0.057957
hsa-miR-4271	0.001784	–	0.057893
hsa-miR-5703	0.003843	–	0.054732
hsa-miR-2114-3p	0.001794	–	0.050406
hsa-miR-1910-3p	0.040831	–	0.049575
hsa-miR-1972	5.90E-06	–	0.045704
hsa-miR-3181	0.001166	–	0.043972
hsa-miR-5571-3p	0.030987	–	0.027284
hsa-miR-409-3p	0.000794	–	0.010936

differentiation, and regulation of smooth muscle cell proliferation. The cellular-component terms associated with hsa-miR-139-5p include RNA polymerase II transcription factor binding (which is involved in the positive regulation of transcription), RNA polymerase II transcription factor binding, mono-saccharide binding, protein heterodimerization activity, protein binding bridging, transcription regulatory region sequence-specific DNA binding, double-stranded DNA binding, GTPase activity, transferase activity, transferring glycosyl groups, and small GTPase regulator activity. The molecular-function terms associated with hsa-miR-139-5p include ruffle, focal adhesion, nuclear chromatin, proteinaceous extracellular matrix, apical part of cell, transcription factor complex, and actin cytoskeleton. Furthermore, hsa-miR-139-5p regulates several pathways, including renal cell carcinoma, pathways in cancer, toll-like receptor signaling, regulation of actin cytoskeleton, and mitogen-activated protein kinase (MAPK)

Table 1 The TNM staging of IRCC and mRCC

Groups	Gender		Age	TNM stage							Stage
	Female	Male		T1 a	T1 b	T2 a	N0	N1	M0	M1	
IRCC	4 (30.76 %)	9 (69.24 %)	67.62 \pm 7.74	7	6	0	13	0	13	0	I
mRCC	5 (33.33 %)	10 (66.67 %)	69.20 \pm 8.83	7	5	3	13	2	0	15	IV

signaling (Fig. 1a). Similarly, hsa-miR-140-3p, hsa-miR-151a-3p, and hsa-miR-204-5p, and hsa-miR-409-3p, hsa-miR-671-3p, hsa-miR-1203, and hsa-miR-1290, are associated with several significant GO functions and KEGG pathways (Fig. 1a, b).

Identification of 214 up-regulated mRNAs and 156 down-regulated mRNAs by mRNA gene-chip analysis

As shown in Table 3, the IRCC and mRCC often occurred in male and reached 80.00 and 60.00 %, respectively, and had no difference in age and gender. According to the TNM staging, the IRCC patient was in T1, N0, and M0, and was divided into I stage, and that of mRCC patients was in T1, T2, N, and M1 and was divided into IV stage.

As indicated by mRNA gene-chip analysis, when compared to mRNAs from patients with IRCC, 214 mRNAs were up-regulated and 156 mRNAs were down-regulated in patients with mRCC. Table 4 shows the top 10 significantly up-regulated and the top 10 significantly down-regulated mRNAs. The up-regulated mRNAs are associated with the biological processes of protein localization to kinetochore, response to salt stress, translesion synthesis, diaphragm, attachment of spindle microtubule to kinetochore, male meiosis, mesonephric tubule development, regulation of respiratory gaseous exchange, and cellular response to gonadotropin stimulus. The cellular-component terms associated with the up-regulated mRNAs include delta DNA polymerase complex, condensed nuclear chromosome, centromeric region, anchored to the membrane, ionotropic glutamate receptor complex, cortical actin cytoskeleton, voltage-gated calcium channel complex, spindle pole, filopodium, sarcoplasmic reticulum, and acrosomal vesicle. The molecular-function terms associated with the up-regulated mRNAs include heparan sulfate proteoglycan binding, DNA-directed DNA polymerase activity, glucuronosyl transferase activity, glutamate receptor activity, voltage-gated calcium channel activity, steroid binding, methylated histone residue binding, cell adhesion molecule binding, S-adenosylmethionine-dependent methyltransferase activity, and sequence-specific DNA binding. Furthermore, the up-regulated mRNAs are associated with KEGG pathways involved in maturity onset diabetes of the young, hypertrophic cardiomyopathy, dilated cardiomyopathy, amyotrophic lateral sclerosis, arrhythmogenic right ventricular cardiomyopathy, rheumatoid arthritis, Alzheimer's disease, cardiac muscle contraction, adipocytokine signaling pathway, hematopoietic cell lineage, T cell receptor signaling pathway, tight junction, neuroactive ligand–receptor interaction, ABC transporters, cytokine–cytokine receptor interaction, MAPK signaling pathway, steroid hormone biosynthesis, drug metabolism–cytochrome P450, purine metabolism, and pyrimidine metabolism (Fig. 2a). Similarly, all the down-regulated mRNAs are associated with the biological processes

Fig. 1 GO and KEGG pathway enrichment of differentially expressed miRNAs after metastasis of renal cell carcinoma. **a** GO and KEGG pathway enrichment of four up-regulated miRNAs. **b** GO and KEGG pathway enrichment of four down-regulated miRNAs

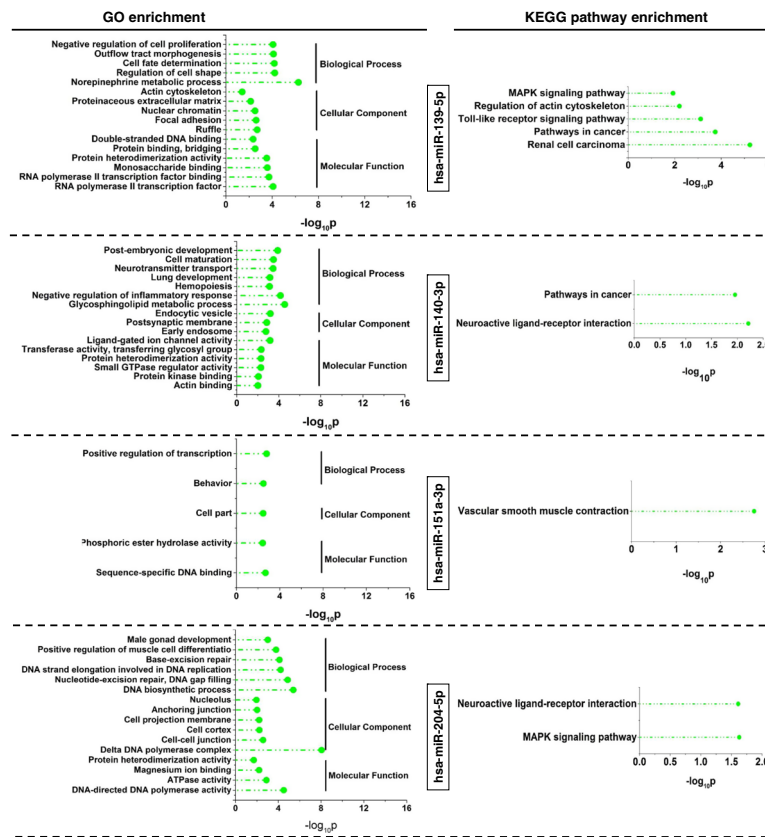
of negative regulation of protein autophosphorylation, norepinephrine metabolic process, dendritic cell differentiation, cellular response to vascular endothelial growth factor stimulus, response to fluid shear stress, negative regulation of cell proliferation, cellular response to cAMP, erythrocyte development, regulation of cell shape, and organ growth. The down-regulated mRNAs are associated with the cellular-component terms T-tubule, ruffle, proteinaceous extracellular matrix, extrinsic to internal side of plasma membrane, postsynaptic membrane, endoplasmic reticulum–Golgi intermediate compartment, transcriptional repressor complex, microvillus, transcription factor complex, postsynaptic density, integral to plasma membrane, focal adhesion, cation channel complex, nuclear chromatin, and endocytic vesicle. The down-regulated mRNAs are associated with the molecular-function terms Rho GTPase activator activity, RNA polymerase II core promoter proximal region sequence-specific DNA binding transcription factor activity involved in positive regulation of transcription, RNA polymerase II transcription factor binding, inward rectifier potassium channel activity, enhancer sequence-specific DNA binding, core promoter proximal region sequence-specific DNA binding, and RNA polymerase II transcription factor binding transcription factor activity involved in positive regulation of transcription. Furthermore, the down-regulated mRNAs are associated with KEGG pathways involved in renal cell carcinoma, pathways in cancer, vascular smooth muscle contraction, GnRH signaling, toll-like receptor signaling, MAPK signaling, Jak–STAT signaling, and glutathione metabolism (Fig. 2b).

Regulatory network includes 1315 miRNA–mRNA pairs

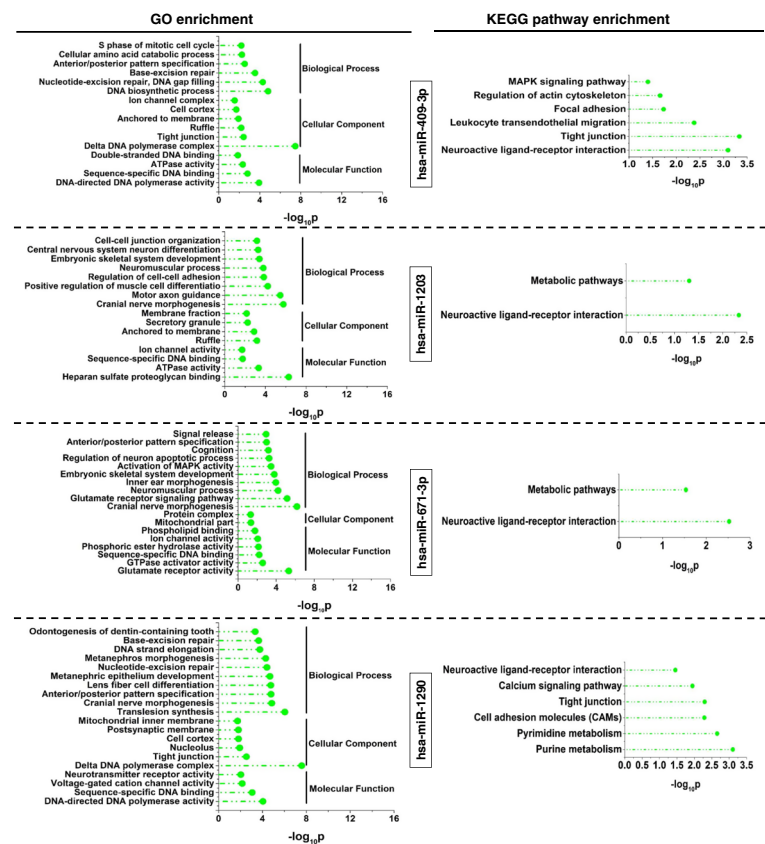
After establishing the regulatory network, 1315 miRNA–mRNA pairs were identified that involved 34 miRNAs and 225 mRNAs. Of these, six miRNA–mRNA pairs were experimentally validated and 1309 pairs were predicted by multiple software programs (Table 5). The miRNA–mRNA regulatory network is shown in Fig. 3.

Significant up-regulation of hsa-miR-140-3p and hsa-miR-151a-3p, and down-regulation of hsa-miR-671-3p and hsa-miR-1290, after metastasis of renal cell carcinoma

The levels of four up-regulated miRNAs, hsa-miR-139-5p, hsa-miR-140-3p, hsa-miR-151a-3p, and hsa-miR-204-5p, and four down-regulated miRNAs, hsa-miR-409-3p, hsa-miR-671-3p, hsa-miR-1203, and hsa-miR-



(A)



(B)

Table 3 The TNM staging of IRCC and mRCC

Groups	Gender		Age	TNM stage							
	Female	Male		T1 a	T1 b	T2 a	N0	N1	M0	M1	Stage
IRCC	1 (20.00 %)	4 (80.00 %)	71.80 ± 8.32	2	3	0	5	0	5	0	I
mRCC	2 (40.00 %)	3 (60.00 %)	69.40 ± 7.20	7	5	3	4	1	0	5	IV

1290, were measured by RT-qPCR. The sequences of the miRNAs and the primers used for amplification are shown in Table 6. In tissues where renal cell carcinoma metastasis occurred, the expressions of all four up-regulated miRNAs were significantly increased when compared to expression in tissues affected by IRCC (** $p < 0.01$; Fig. 4). Of the four up-regulated miRNAs, hsa-miR-140-3p and hsa-miR-151a-3p were chosen to screen for target genes. Similarly, the expressions of the four down-regulated miRNAs were

significantly decreased when compared to expression in tissues affected by IRCC (** $p < 0.01$; Fig. 4). Of the four down-regulated miRNAs, hsa-miR-671-3p and hsa-miR-1290 were chosen to screen for target genes.

Expressions of NEU2, MASP1, and MCL1 are significantly affected after renal cell carcinoma metastasis

Based on the sequences of the up-regulated miRNAs hsa-miR-140-3p and hsa-miR-151a-3p, and the down-

Table 4 Differentially expressed mRNAs in patients compared mRCC with IRCC

Gene ID	<i>p</i> value	Direction	FC	Gene symbol	Gene description
317,701	0.02037	+	20.7192635	VN1R2	Vomeronal 1 receptor 2
121,599	0.00273	+	12.84124468	SPIC	Spi-C transcription factor (Spi-1/PU.1 related)
3198	0.01439	+	12.76072124	HOXA1	Homeobox A1
9073	0.02852	+	12.49742492	CLDN8	Claudin 8
27,136	0.0003	+	12.3389332	MORC1	MORC family CW-type zinc finger 1
150,197	0.01752	+	11.9592022	LOC150197	Uncharacterized LOC150197
90,499	0.02431	+	11.77113183	LOC90499	Uncharacterized LOC90499
9824	0.04965	+	11.19855685	ARHGAP11A	Rho GTPase-activating protein 11A
390,892	0.01578	+	11.10234779	OR7A10	Olfactory receptor, family 7, subfamily A, member 10
5969	0.00105	+	11.09129826	REG1P	Regenerating islet-derived 1 pseudogene
7288	0.02854	-	0.110791896	TULP2	Tubby-like protein 2
149,018	0.04442	-	0.110654921	LELP1	Late cornified envelope-like proline-rich 1
646,736	0.00359	-	0.099475388	LOC646736	Uncharacterized LOC646736
100,507,533	0.00211	-	0.08456666	SOX21-AS1	SOX21 antisense RNA 1 (non-protein coding)
729,234	0.00063	-	0.076463914	FAHD2CP	Fumarylacetoacetate hydrolase domain containing 2C, pseudogene
166,752	0.01905	-	0.075749791	FREM3	FRAS1-related extracellular matrix 3
400,966	0.00185	-	0.063266293	RGPD1	RANBP2-like and GRIP domain containing 1
645,485	0.00056	-	0.043853468	LOC645485	Uncharacterized LOC645485
387,755	0.04315	-	0.116443038	INSC	Inscuteable homolog (<i>Drosophila</i>)
100,507,190	0.0279	-	0.113832127	LOC100507190	Uncharacterized LOC100507190

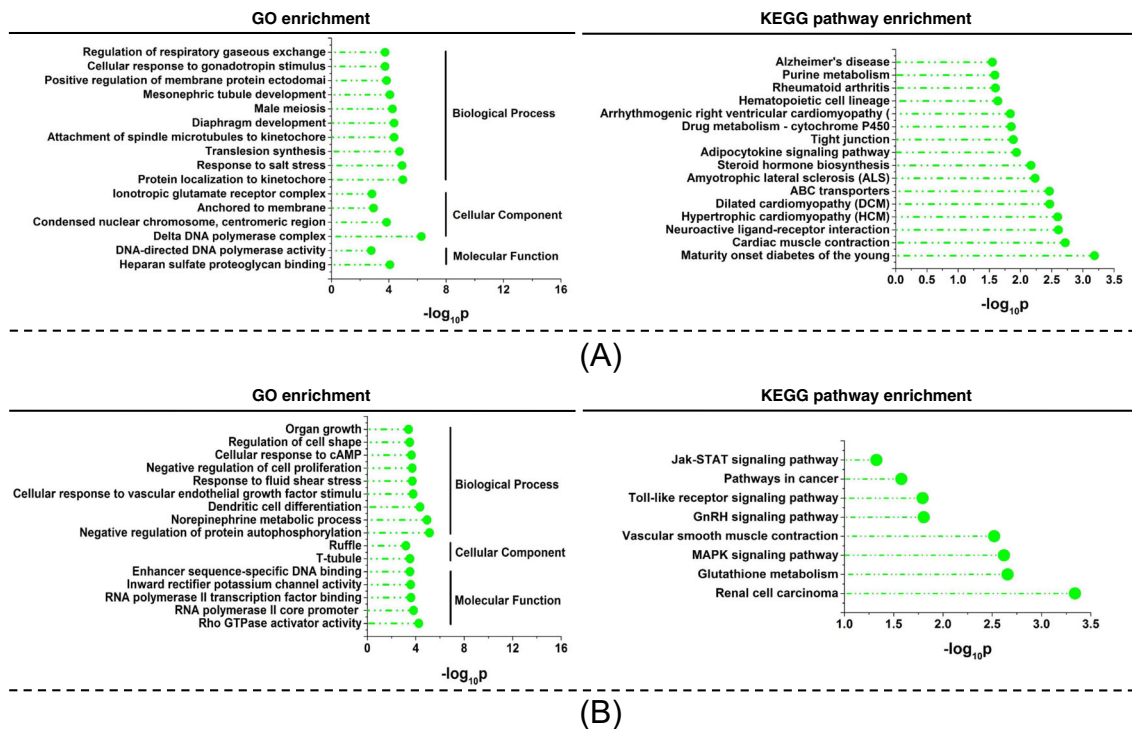


Fig. 2 GO and KEGG pathway enrichment of differentially expressed mRNAs after metastasis of renal cell carcinoma. **a** GO and KEGG pathway enrichment of four up-regulated mRNAs. **b** GO and KEGG pathway enrichment of four down-regulated mRNAs

regulated miRNAs hsa-miR-671-3p and hsa-miR-1290, the expressions of the target genes *NEU2*, *MASPI*,

MCL1, *ARHGAP11A*, *HOXA1*, and *CLDN8* were analyzed by RT-qPCR. The sequences of the mRNAs and

Table 5 miRNA-mRNA pairs in patients compared mRCC with IRCC

microRNA	Gene ID	Gene symbol	Gene description	FC of miRNA (FC1)	FC of gene (FC2)	θ (FC2/FC1)
hsa-miR-507	400,966	RGPD1	RANBP2-like and GRIP domain containing 1	2.337247909	0.063266293	6.76274222
hsa-miR-1291	9073	CLDN8	Claudin 8	0.478492306	12.49742492	5.979921668
hsa-miR-486-3p	9073	CLDN8	Claudin 8	0.462953319	12.49742492	5.785724345
hsa-miR-133b	3198	HOXA1	Homeobox A1	0.423333102	12.76072124	5.402035706
hsa-miR-486-3p	9824	ARHGAP11A	Rho GTPase-activating protein 11A	0.462953319	11.19855685	5.184409062
hsa-miR-1291	4107	MAGEA8	Melanoma antigen family A, 8	0.478492306	10.22264691	4.891457894
hsa-miR-486-3p	29,114	TAGLN3	Transgelin 3	0.462953319	10.29079772	4.764158958
hsa-miR-133b	9824	ARHGAP11A	Rho GTPase-activating protein 11A	0.423333102	11.19855685	4.74071981
hsa-miR-486-3p	4640	MYO1A	Myosin IA	0.462953319	9.796660997	4.535396724
hsa-miR-1291	57,111	RAB25	RAB25, member RAS oncogene family	0.478492306	9.215066527	4.409338432
hsa-miR-486-3p	57,111	RAB25	RAB25, member RAS oncogene family	0.462953319	9.215066527	4.266145633
hsa-miR-647	390,892	OR7A10	Olfactory receptor, family 7, subfamily A, member 10	0.380947676	11.10234779	4.229413589
hsa-miR-1246	121,599	SPIC	Spi-C transcription factor (Spi-1/PU.1 related)	0.321340717	12.84124468	4.126414773
hsa-miR-1246	3198	HOXA1	Homeobox A1	0.321340717	12.76072124	4.100539312
hsa-miR-1291	56,155	TEX14	Testis expressed 14	0.478492306	8.508523165	4.07126287
hsa-miR-1246	9073	CLDN8	Claudin 8	0.321340717	12.49742492	4.015931484
hsa-miR-647	4107	MAGEA8	Melanoma antigen family A, 8	0.380947676	10.22264691	3.894293583
hsa-miR-1291	9028	RHBDL1	Rhomboid, veinlet-like 1 (<i>Drosophila</i>)	0.478492306	7.97221429	3.814643199
hsa-miR-486-3p	9028	RHBDL1	Rhomboid, veinlet-like 1 (<i>Drosophila</i>)	0.462953319	7.97221429	3.690763065

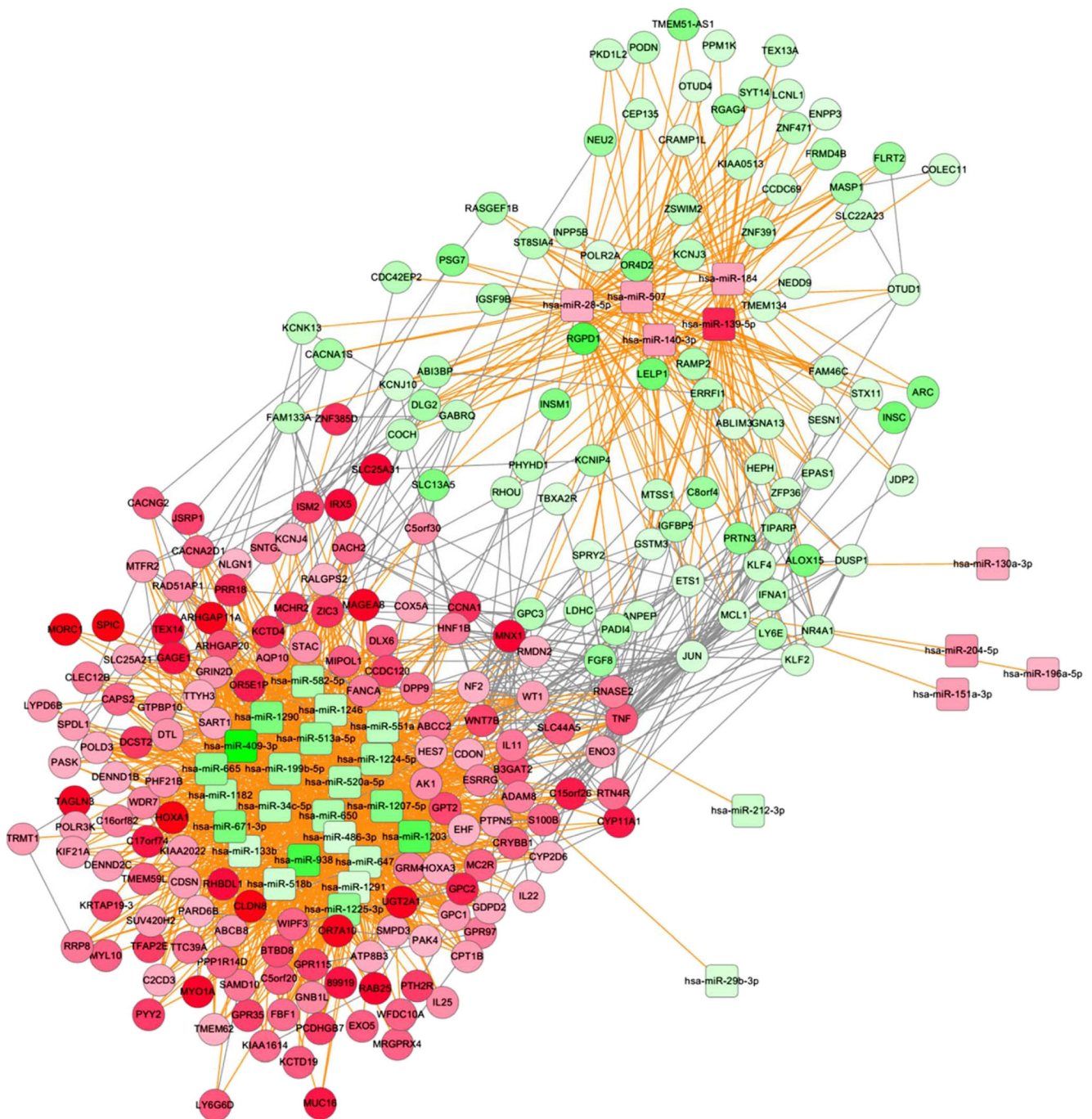


Fig. 3 miRNA-mRNA regulatory network established by bioinformatic approaches. The figure shows the 1315 miRNA-mRNA pairs obtained, which involve 34 miRNAs and 225 mRNAs

the primers used for amplification are shown in Table 7. After renal cell carcinoma metastasis, the expressions of *NEU2*, *MASP1*, and *MCL1* were significantly decreased, and the expressions of *ARHGAP11A*, *HOXA1*, and *CLDN8* were significantly increased when compared to expression in tissues affected by IRCC ($*p < 0.05$, $**p < 0.01$; Fig. 5).

miRNAs hsa-miR-140-3p, hsa-miR-151a-3p, hsa-miR-671-3p, and hsa-miR-1290 significantly down-regulate their target genes by binding to the 3'-UTR of their mRNAs

In a dual-luciferase reporter gene assay (Fig. 6), after cotransfecting cells with hsa-miR-140-3p mimic and

Table 6 Sequences of miRNAs and primers used for qRT-PCR amplification

miRNA and sequences		Primer sequences
hsa-miR-139-5p (MIMAT0000250)	UCUACAGUGCACGUGUCUCCAGU	5'-GCTCGGTCTACAGTGCACGT-3'/5'-CACTTCCTCAGCACTTGTGGTAT-3'
hsa-miR-140-3p (MIMAT0004597)	UACCACAGGGUAGAACCACGG	5'-CAGTGTGTACCACAGGGTAGA-3'/5'-CACTTCCTCAGCACTTGTTCCTAT-3'
hsa-miR-151a-3p (MIMAT0000757)	CUAGACUGAAGCUCCUUGAGG	5'-AGTGCTGCTAGACTGAAGCTCC-3'/5'-CACATCCTCAGCACTTGTGGTAT-3'
hsa-miR-204-5p (MIMAT0000265)	UUCCCUUUGUCAUCCU AUGCCU	5'-CTGCCGTTCCCTTTGTCAT-3'/5'-CTCTGTCTCTCGTCTTGTGGT AT-3'
hsa-miR-409-3p (MIMAT0001639)	GAAUGUUGCUCGGUGAACCCCU	5'-AGTGTGGAATGTTGCTCGG-3'/5'-CACTTCCTCAGCACTTGTGGTAT-3'
hsa-miR-1203 (MIMAT0005866)	CCCGGAGCCAGGAUGCAGCUC	5'-AGTATTACCCGGAGCCAGGA-3'/5'-CACTTCCTCAGCACTTGTGGTAT-3'
hsa-miR-671-3p (MIMAT0004819)	UCCGGUUCUCAGGGCUCCACC	5'-AGTGCTGTCCGGTCTCAGG-3'/5'-CACTTCCTCAGCACTTGTGGTAT-3'
hsa-miR-1290 (MIMAT0005880)	UGGAUUUUUGGAUCAGGGA	5'-CAGTGTGTGGATTTTTGGAT-3'/5'-CACTTCCTCAGCACTTGTGGTAT-3'

psiCHECK-2-UTR (*MASPI*), the ratio of firefly luciferase/*Renilla* luciferase significantly decreased (***p* < 0.01) and was restored to normal after cotransfecting hsa-miR-140-3p

mimic, inhibitor, and psiCHECK-2-UTR (*MASPI*). However, hsa-miR-140-3p mimic had no effect on the 3'-UTR of *NEU2*. Similarly, after cotransfecting hsa-miR-151a-3p mimic and

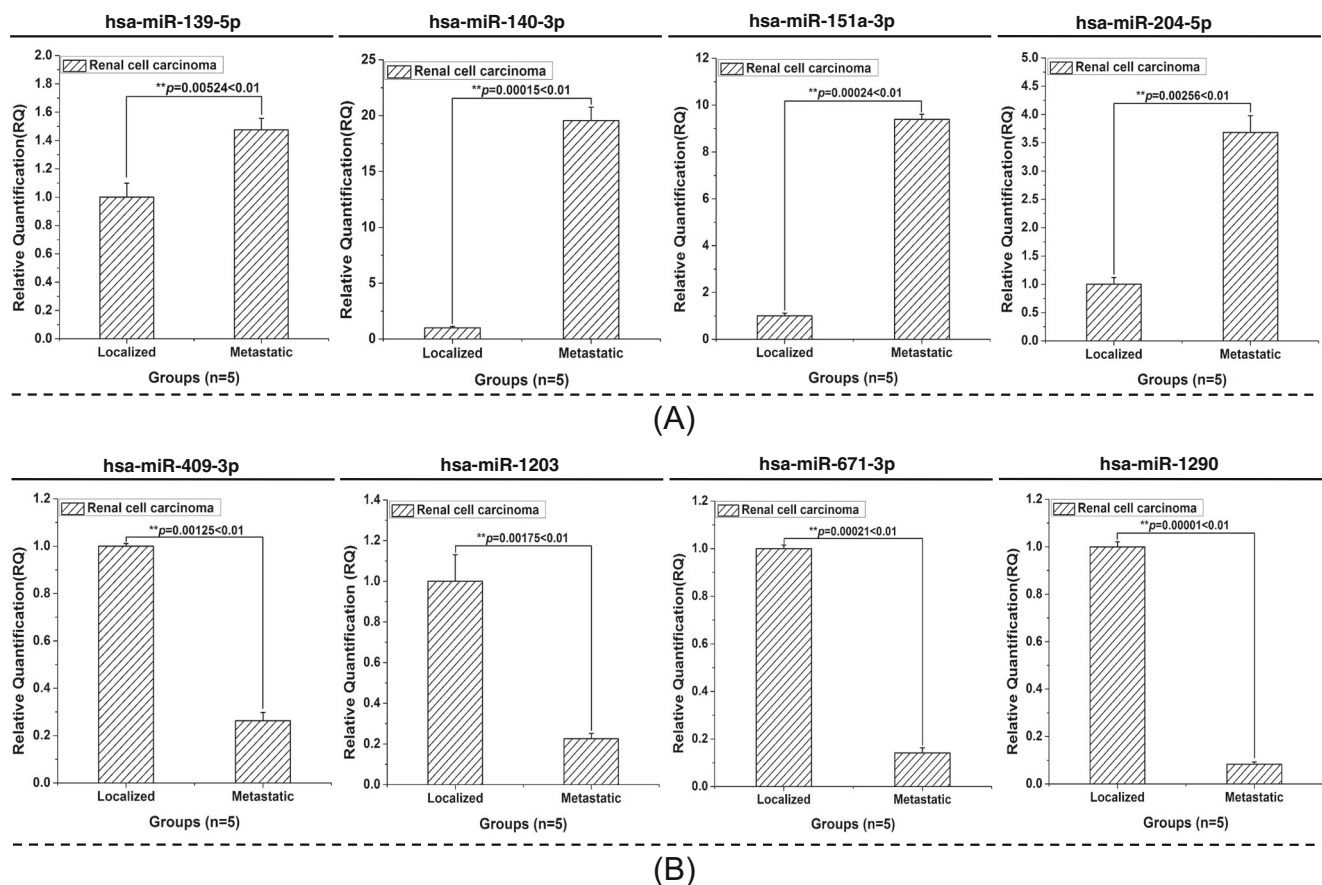


Fig. 4 Identification of differentially expressed miRNAs by quantitative reverse transcription PCR (RT-qPCR). **a** Identification of four up-regulated miRNAs. **b** Identification of four down-regulated miRNAs.

The expression level of miRNAs as determined by RT-qPCR is consistent with that determined by miRNA gene-chip analysis

Table 7 Sequences of mRNAs and primers used for qRT-PCR amplification

Gene ID	Gene name	Primer sequences
4759	NEU2	5'-AGTGGCAAGCTCAGGAGGTGGT-3'/ 5'-TGGTCTGCAGCTGCTGTTGCTC-3'
5648	MASP1	5'-AACCCATCAGCACCCAGAGCCA-3'/ 5'-TGGGCACTCATTTCCTGCAGCC-3'
4170	MCL1	5'-AAAGCCAATGGGCAGGTCTGGG-3'/ 5'-CCCAGTTTGTTACGCCGTCGCT-3'
9824	ARHGAP11A	5'-ACTCCTGTTTCGTAGTCCGTC-3'/5'- AGCACCGTCACAGCTCACTGAT-3'
3198	HOXA1	5'-TCCAGAACCGCCGAATGAAGCA-3'/ 5'-TTCCTCGCCTTCTCGTCGTTT-3'
9073	CLDN8	5'-AGGTGCACGGGGACAATGAGA-3'/ 5'-TGGCAACCCAGCTCACAGGGAT-3'
345,651	β -actin	5'-ATAACCCTGGCACCCAGCACCA- 3'/5'-TGGACAGGCTGGCAAGGATG GA-3'

psiCHECK-2-UTR (*MCL1*), hsa-miR-671-3p mimic and psiCHECK-2-UTR (*HOXA1*), and hsa-miR-1290 mimic and psiCHECK-2-UTR (*HOXA1*), the ratios of firefly luciferase/*Renilla* luciferase significantly decreased (** $p < 0.01$). However, the hsa-miR-671-3p mimic did not regulate the 3'-UTR of *ARHGAP11A*, and hsa-miR-1290 mimic did not regulate the 3'-UTR of *CLDN8*.

Discussion

In this study, as expected, several differentially expressed miRNAs and mRNAs were identified by miRNA gene-chip and mRNA gene-chip analyses, 31 up-regulated miRNAs, 196 down-regulated miRNAs, 214 up-regulated mRNAs, and 156 down-regulated mRNAs. Their regulatory network included 1315 miRNA-mRNA pairs. After the metastasis of renal cell carcinoma, the expressions of several miRNAs, including hsa-

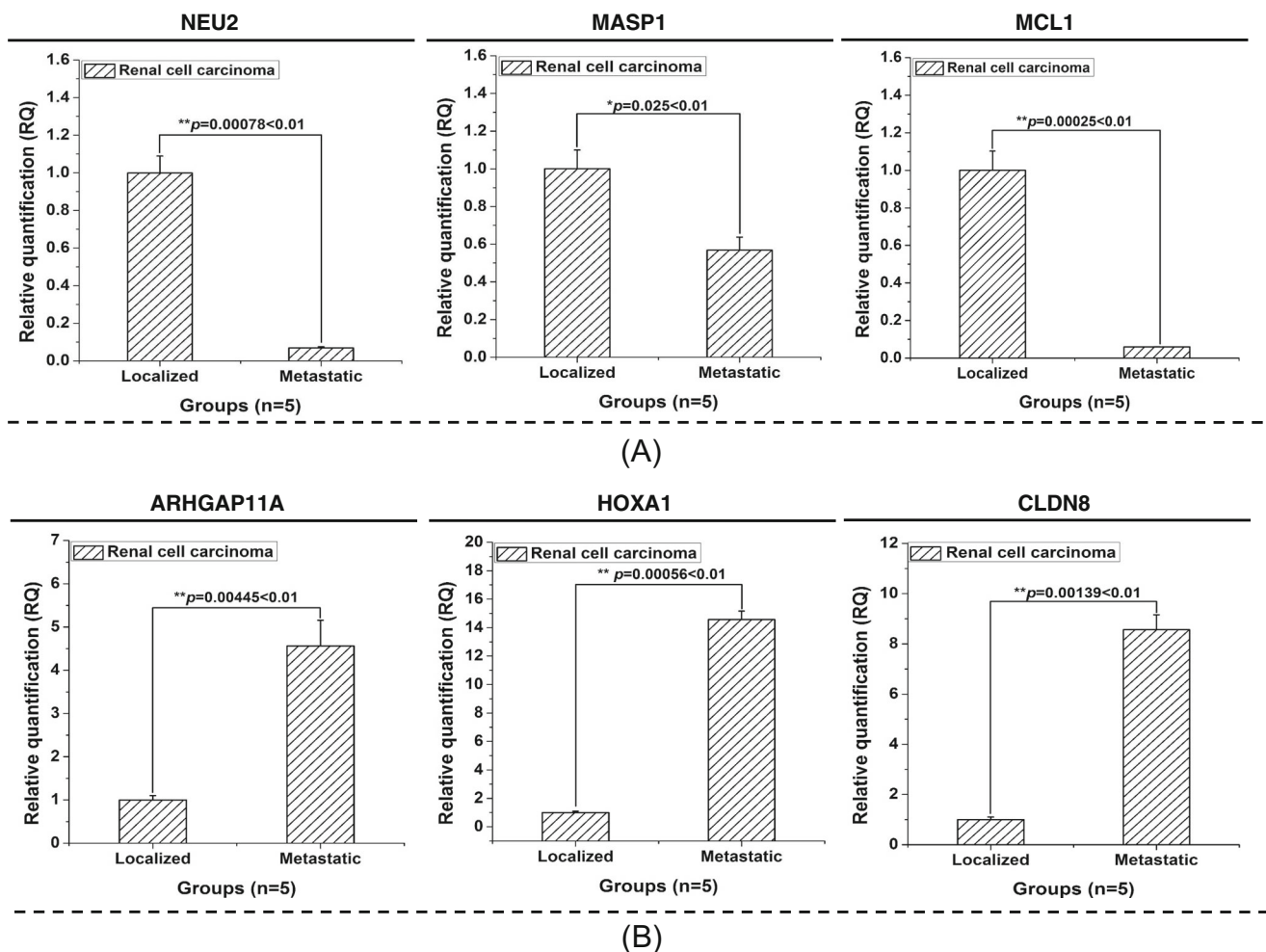


Fig. 5 Identification of differentially expressed mRNAs by quantitative reverse transcription PCR. **a** Identification of the expressions of *NEU2*, *MASP1*, and *MCL1* genes by quantitative reverse transcription PCR. **b** Identification of the expressions of *ARHGAP11A*, *HOXA1*, and *CLDN8*

genes by quantitative reverse transcription PCR. Expressions of *NEU2*, *MASP1*, and *MCL1* are decreased, and expressions of *ARHGAP11A*, *HOXA1*, and *CLDN8* are increased (* $p < 0.05$, ** $p < 0.01$)

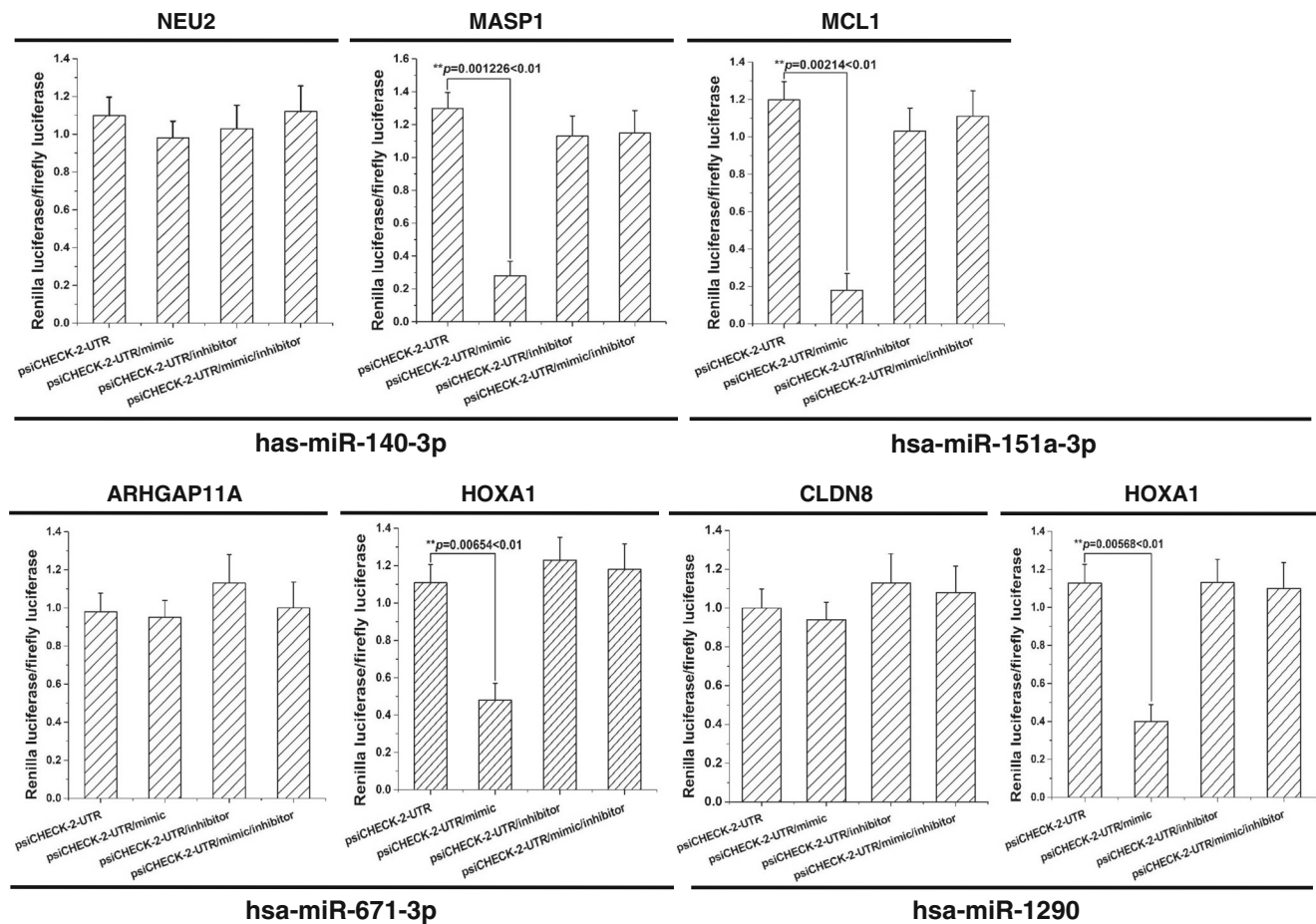


Fig. 6 Dual-luciferase reporter gene assay of miRNAs and their targets. The hsa-miR-140-3p miRNA binds to the 3'-UTR of the *MASP1* mRNA to decrease its expression, and hsa-miR-151a-3p, hsa-miR-671-3p, and hsa-miR-1290 similarly bind to their target mRNAs

miR-139-5p, hsa-miR-140-3p, hsa-miR-151a-3p, and hsa-miR-204-5p, and of several mRNAs, including hsa-miR-409-3p, hsa-miR-671-3p, hsa-miR-1203, and hsa-miR-1290, were affected, as demonstrated by RT-qPCR results that were consistent with the results of miRNA gene-chip analysis. Likewise, the expressions of several mRNAs, including *NEU2*, *MASP1*, *MCL1*, *ARHGAP11A*, *HOXA1*, and *CLDN8*, were similarly regulated. In an in vitro experiment, hsa-miR-140-3p bound to the 3'-UTR of *MASP1* and decreased *MASP1* expression, and hsa-miR-151a-3p, hsa-miR-671-3p, and hsa-miR-1290 bound to the 3'-UTRs to negatively regulate their target genes.

Several studies have shown that miRNAs specifically regulate gene expression in cells to control a number of biological functions, such as development, anti-viral defense, hematopoiesis, organ specificity, cell proliferation, apoptosis, fat metabolism, and cancer genesis and development. In particular, the influence of miRNAs on cancer genesis and development, and their potential curative effects, have become the focus of recent studies [27]. For example, miR-155 directly targets the *VHL* mRNA to accelerate the activation of the hypoxia-inducible factor signaling pathway and revascularization [28]; miR-29b indirectly regulates VEGF expression in renal

cell carcinoma and regulates the expression of *TIS11B* [29]; elevated levels of miR-205 down-regulate the expressions of the *SRC*, *LYN*, and *YES1* genes to inhibit the proliferation of renal cell carcinoma [30]; and the combined up-regulation of miR-155 and down-regulation of miR-141 distinguishes normal renal tissue from renal carcinoma with an accuracy of approximately 97 % [31]. Therefore, more studies have focused on miRNAs as biomarkers for renal cell carcinoma genesis and development and as having potential clinical applications. Importantly, recent studies have focused on a limited number of miRNAs in renal carcinoma, and there has not yet been a large-scale study using gene-chip analysis. In this study, miRNA and mRNA gene-chip analyses were carried out, with the goals of screening a larger number of differentially expressed miRNAs and mRNAs and of identifying more miRNA-mRNA pairs in mRCC.

In this study, differentially expressed miRNAs, 31 up-regulated and 196 down-regulated miRNAs, were identified by miRNA gene-chip analysis. Based on significant differences and no reporting in mRCC versus IRCC, four up-regulated and four down-regulated miRNAs were selected as candidates for validation by RT-qPCR. Although these

miRNAs have not previously been associated with renal cell carcinoma or mRCC, they have been reported to be closely associated with the genesis and development of cancers, including liver cancer, gastric cancer, and lung cancer. For instance, hsa-miR-140-3p is a biomarker for squamous cell carcinoma [32]. The change in expression of the selected miRNAs measured by RT-qPCR was consistent with the results from miRNA gene-chip analysis; hsa-miR-140-3p and hsa-miR-151a-3p were significantly up-regulated, and hsa-miR-671-3p and hsa-miR-1290 were significantly down-regulated. Therefore, these four miRNAs were used to screen for RNA targets by RT-qPCR. The expression levels of *NEU2*, *MASPI*, *MCL1*, *ARHGAP11A*, *HOXA1*, and *CLDN8* were consistent with those observed by mRNA gene-chip analysis and indicated that the four candidate miRNAs regulate their target genes by binding to the 3'-UTRs of their mRNAs. As expected, hsa-miR-140-3p bound to the 3'-UTR of *MASPI* and decreased its expression, and hsa-miR-151a-3p, hsa-miR-671-3p, and hsa-miR-1290 similarly bound to their target mRNAs and significantly down-regulated their expressions in vitro. These results indicated that hsa-miR-140-3p, hsa-miR-151a-3p, hsa-miR-671-3p, and hsa-miR-1290 may be developed as a potential therapeutic target for mRCC via down-regulation of their target mRNAs, and however this study just a pilot study, and numerous investigations need to validate in the future work, such as cell proliferation, cell cycle, cell apoptosis, cell migration, and invasion.

The present study confirmed the presence of a miRNA-mRNA crossover network by using gene chips, bioinformatic analyses, and molecular biology experiments. However, additional miRNAs and mRNAs need to be evaluated. Because of the limited sample size, the variability of the data was large and unstable. In order to exclude individual differences, miRNAs and mRNAs from many more mRCC cases need to be studied to reduce experimental error.

Acknowledgments This work was financially supported by the National Natural Science Foundation of China (no. 81100483) and the National High Technology Research and Development Program of China (863 program; no. 2012AA021100).

References

- Torre LA, Bray F, Siegel RL, Ferlay J, Lortet-Tieulent J, Jemal A. Global cancer statistics, 2012. *CA Cancer J Clin*. 2015;65:87–108.
- Siegel RL, Miller KD, Jemal A. Cancer statistics, 2015. *CA Cancer J Clin*. 2015;65:5–29.
- Chow WH, Devesa SS, Warren JL, Fraumeni Jr JF. Rising incidence of renal cell cancer in the United States. *JAMA*. 1999;281:1628–31.
- Fenaux P, Haase D, Sanz GF, Santini V, Buske C. Myelodysplastic syndromes: ESMO clinical practice guidelines for diagnosis, treatment and follow-up. *Ann Oncol*. 2014;25(Suppl 3):iii57–69.
- Glynn-Jones R, Nilsson PJ, Aschele C, Goh V, Peiffert D, Cervantes A, Arnold D. Anal cancer: ESMO-ESSO-ESTRO clinical practice guidelines for diagnosis, treatment and follow-up. *Eur J Surg Oncol*. 2014;40:1165–76.
- Gastrointestinal stromal tumours: ESMO clinical practice guidelines for diagnosis, treatment and follow-up. *Ann Oncol*. 2014;25 Suppl 3:iii21–26.
- Dreyling M, Ghielmini M, Marcus R, Salles G, Vitolo U, Ladetto M. Newly diagnosed and relapsed follicular lymphoma: ESMO clinical practice guidelines for diagnosis, treatment and follow-up. *Ann Oncol*. 2014;25(Suppl 3):iii76–82.
- Bozkurt O, Karaca H, Hacibekiroglu I, Kaplan MA, Duzkopru Y, Uysal M, Berk V, Inanc M, Duran AO, Ozaslan E, Ucar M, Ozkan M. Is sunitinib-induced hypothyroidism a predictive clinical marker for better response in metastatic renal cell carcinoma patients? *J Chemother*. 2015;1973947815Y0000000039.
- Diekstra MH, Swen JJ, Boven E, Castellano D, Gelderblom H, Mathijssen RH, Rodriguez-Antona C, Garcia-Donas J, Rini BI, Guchelaar HJ. Cyp3a5 and abcb1 polymorphisms as predictors for sunitinib outcome in metastatic renal cell carcinoma. *Eur Urol*. 2015.
- Miyazaki A, Miyake H, Harada K, Fujisawa M. No significant correlation of clinical outcomes between first- and second-line tyrosine kinase inhibitors in patients with metastatic renal cell carcinoma. *Anticancer Res*. 2015;35:3067–73.
- Laitinen M, Parry M, Ratasvuori M, Wedin R, Albergo JJ, Jeys L, Abudu A, Carter S, Gaston L, Tillman R, Grimer R. Survival and complications of skeletal reconstructions after surgical treatment of bony metastatic renal cell carcinoma. *Eur J Surg Oncol*. 2015.
- Bodnar L, Stec R, Cierniak S, Synowiec A, Weislo G, Jesiotr M, Koktyz R, Kozłowski W, Szczylik C. Clinical usefulness of PI3K/Akt/mTOR genotyping in companion with other clinical variables in metastatic renal cell carcinoma patients treated with everolimus in the second and subsequent lines. *Ann Oncol*. 2015.
- Abdallah AO, Vallurupalli S, Kunthur A. Pazopanib- and bevacizumab-induced reversible heart failure in a patient with metastatic renal cell carcinoma: a case report. *J Oncol Pharm Pract*. 2015.
- Lamuraglia M, Raslan S, Elaidi R, Oudard S, Escudier B, Slimane K, Penna RR, Wagner M, Lucidarme O. mTOR-inhibitor treatment of metastatic renal cell carcinoma: contribution of Choi and modified Choi criteria assessed in 2D or 3D to evaluate tumor response. *Eur Radiol*. 2015.
- Wang CH, Zhao TX, Li M, Zhang C, Xing XH. Characterization of a novel acinetobacter baumannii xanthine dehydrogenase expressed in *Escherichia coli*. *Biotechnol Lett*. 2015.
- Wu D, Gantier MP. Normalization of affymetrix miRNA microarrays for the analysis of cancer samples. *Methods Mol Biol*. 2015.
- Berezikov E, Guryev V, van de Belt J, Wienholds E, Plasterk RH, Cuppen E. Phylogenetic shadowing and computational identification of human microRNA genes. *Cell*. 2005;120:21–4.
- Croce CM. Causes and consequences of microRNA dysregulation in cancer. *Nat Rev Genet*. 2009;10:704–14.
- Juan D, Alexe G, Antes T, Liu H, Madabhushi A, Delisi C, Ganesan S, Bhanot G, Liou LS. Identification of a microRNA panel for clear-cell kidney cancer. *Urology*. 2010;75:835–41.
- Yi Z, Fu Y, Zhao S, Zhang X, Ma C. Differential expression of miRNA patterns in renal cell carcinoma and nontumorous tissues. *J Cancer Res Clin Oncol*. 2010;136:855–62.
- Qiu ZL, Shen CT, Song HJ, Wei WJ, Luo QY. Differential expression profiling of circulation microRNAs in PTC patients with non-(131)I and (131)I-avid lungs metastases: a pilot study. *Nucl Med Biol*. 2015;42:499–504.
- Zhang J, Liu Y, Liu Z, Wang XM, Yin DT, Zheng LL, Zhang DY, Lu XB. Differential expression profiling and functional analysis of

- microRNAs through stage I-III papillary thyroid carcinoma. *Int J Med Sci.* 2013;10:585–92.
23. Chow TF, Youssef YM, Lianidou E, Romaschin AD, Honey RJ, Stewart R, Pace KT, Yousef GM. Differential expression profiling of microRNAs and their potential involvement in renal cell carcinoma pathogenesis. *Clin Biochem.* 2010;43:150–8.
 24. Butz H, Szabo PM, Khella HW, Nofech-Mozes R, Patocs A, Yousef GM. MiRNA-target network reveals miR-124as a key miRNA contributing to clear cell renal cell carcinoma aggressive behaviour by targeting CAV1 and FLOT1. *Oncotarget.* 2015;6:12543–57.
 25. Wittekind C, Oberschmid B. TNM classification of malignant tumors 2010: general aspects and amendments in the general section. *Pathologe.* 2010;31:333–4 .336-338
 26. Wittekind C. 2010 TNM system: on the 7th edition of TNM classification of malignant tumors. *Pathologe.* 2010;31:331–2.
 27. Selbach M, Schwanhausser B, Thierfelder N, Fang Z, Khanin R, Rajewsky N. Widespread changes in protein synthesis induced by microRNAs. *Nature.* 2008;455:58–63.
 28. Tili E, Michaille JJ, Wernicke D, Alder H, Costinean S, Volinia S, Croce CM. Mutator activity induced by microRNA-155 (miR-155) links inflammation and cancer. *Proc Natl Acad Sci U S A.* 2011;108:4908–13.
 29. Sinha S, Dutta S, Datta K, Ghosh AK, Mukhopadhyay D. Von Hippel-Lindau gene product modulates tis11b expression in renal cell carcinoma: impact on vascular endothelial growth factor expression in hypoxia. *J Biol Chem.* 2009;284:32610–8.
 30. Majid S, Saini S, Dar AA, Hirata H, Shahryari V, Tanaka Y, Yamamura S, Ueno K, Zaman MS, Singh K, Chang I, Deng G, Dahiya R. MicroRNA-205 inhibits SRC-mediated oncogenic pathways in renal cancer. *Cancer Res.* 2011;71:2611–21.
 31. Jung M, Mollenkopf HJ, Grimm C, Wagner I, Albrecht M, Waller T, Pilarsky C, Johannsen M, Stephan C, Lehrach H, Nietfeld W, Rudel T, Jung K, Kristiansen G. MicroRNA profiling of clear cell renal cell cancer identifies a robust signature to define renal malignancy. *J Cell Mol Med.* 2009;13:3918–28.
 32. Tan X, Qin W, Zhang L, Hang J, Li B, Zhang C, Wan J, Zhou F, Shao K, Sun Y, Wu J, Zhang X, Qiu B, Li N, Shi S, Feng X, Zhao S, Wang Z, Zhao X, Chen Z, Mitchelson K, Cheng J, Guo Y, He J. A 5-microRNA signature for lung squamous cell carcinoma diagnosis and HSA-miR-31 for prognosis. *Clin Cancer Res.* 2011;17:6802–11.